Optimization of Co-Flow Jet Parameters for Ahmed Body Application

Ikram Derghal[1], Mohd Saifuddin[2], Mohd Hafiz Mohd Noh[1], Ahmad Hussein Abdul Hamid[1*]

[1]School of Mechanical Engineering, College of Engineering,
 Universiti Teknologi MARA, 40450 Shah Alam, Selangor, MALAYSIA

[2]Department of Mathematics and Statistics,
 Bangladesh University of Business and Technology, Dhaka, BANGLADESH

*Corresponding Author

Abstract: This study evaluates the drag reduction strategy of suction and blowing on idealize automotive vehicle, Ahmed Body. Optimization approach is adapted in order to analyse the effect of slot location, momentum coefficient and slot angle on the vehicle which experiencing drag. Despite all the efforts that have been done to reduce the Ahmed body drag using various active flow control system, most of the drag reduction were only less than 15%. A 25° Ahmed body with build in co-flow jet is modelled using a CAD software. The flow around the Ahmed body is simulated at Reynolds number based on length Re = 4.29×10^6. The governing equation were solve using an open source software package, which has been validated against experimental data. Pressure Implicit with Splitting of Operator (PISO) algorithm is applied to solve the equation. The outcome of the simulation are varies depending on the variables. Some show a decrease in drag while there are also that actually increase the drag of the system. This are caused by the suction and blowing slots that effect the surrounding air flow whether it is reducing or increasing the wake size downstream of the body. The result shows the momentum coefficient and location of both suction and blowing jet played an important role of manipulating the flow around the body and reducing the drag. The velocity contours indicated that the key to drag reduction is by using 40 m/s jet velocity, placement of suction and blowing away from each other.

Keywords: Ahmed Body, drag reduction, suction, blowing

1. Introduction

Vehicle or automobile are invention made to help mankind travel distances while decreasing the time consumption. Vehicle will be constantly subjected to drag force as it moves. A force causing the vehicle to consume more energy. Reducing drag force on a vehicle will increase the fuel efficiency, hence reduce amount of fuel over the same distance. Ahmed Body is used as a simplified and idealized version of an automobile for the purpose of experimentation and computational calculation, as shown in

. Even in idealize version, there are a lot of aerodynamic drag that will cause more consumption of energy and money. Pressure drag contribute up to 85% of the total drag on a basic Ahmed Body while the other remainder is friction drag med [1].Few flow patterns acting on Ahmed body are forebody separation bubble, c-pillar vortex, backlight, rear spanwise recirculation and lower vortex, these flow pattern can be seen in Figure 1(a) [2]. Finding few ways to decrease the drag force effect will be very beneficial.

The study of drag reduction of road vehicles has been a subject of interest for a quite some time. It has been proven by various researches done on Ahmed body with flow control (whether it is passive flow control or active flow control) that the mechanism to minimize the drag is by delaying or eliminating the flow separation. Despite that, there are still a lot more that can be investigated into the topic of the strategy of drag reduction on Ahmed body, specifically the application of suction and blowing at the rear end of the Ahmed body to minimize the drag occurring there.

The objective for this work is to evaluate the drag reduction strategy of suction and blowing on idealize automotive vehicle, namely Ahmed body. The subsidiary objective is to perform optimization and analyze the effect of the slot location, momentum coefficient and slot angle on the drag experienced by the vehicle. Owing to the fact that, the application of suction and blowing is not widely applied to road vehicle and there are limited studies on the topic, this drag reduction strategy can be taken into consideration into the future of vehicles.

This project will be made to study the flow around a 2-dimensional and 3 dimensional idealize automotive body or Ahmed body. Analyze the method of active flow control strategy of suction and blowing with the intention of reducing aerodynamic drag cause by flow separation. For the numerical solving of the flow, governing equations are in play with an open source CFD package Open Foam for baseline Ahmed body and co-flow jet, CFJ, Ahmed body Reynolds number, $Re = 4.29 \times 10^6$ and the freestream velocity $U0 = 40$ m/s. The independent variable for the parametric CJF study is location of slot, momentum coefficient and angle of injection. Unsteady Reynolds-averaged Navier-Strokes (URANS) and Large Eddy Simulation (LES) of the turbulent flow are applied in the project to calculate the numerical for 2D and 3D respectively.
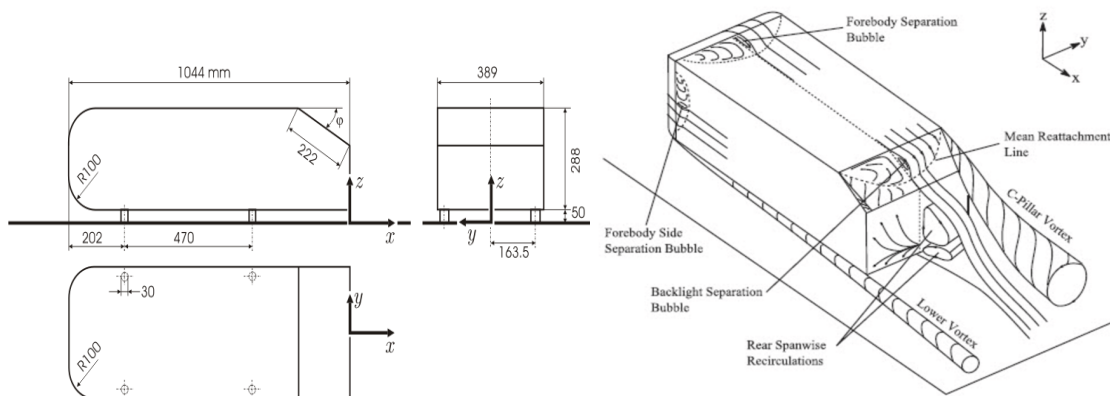

Fig. 1 - (a) Ahmed Body; (b) flow pattern on Ahmed Body model (Ahmed et al. 1984)

2. Literature Review

One-way fluid dynamics can offer to reduce drag is by flow control. Flow control is the manipulation of flow field that will change the outcome [3]. Flow control can be approach in two ways, passive and active flow control systems. Passive flow control system means the flow control do not require auxiliary power and no control loop. Meanwhile, active require energy expenditure [4]. In passive flow control, there are few methods that exist which are retrofits, control surface and design modifications. The advantage of using passive is that the simplicity, cost effectiveness and easier implementation compared to active flow control [5]. Meanwhile, the advantage of active flow control over passive is the technology advancement and using localized, small energy input the flow can cause a massive effect by controlling the natural stability of controlling complex, dynamical processes like turbulence production in turbulent boundary layers to reduce skin friction and hence viscous drag are an active flow functionality.

In active flow control, suction is where the weak boundary layer of a body which because drag is sucked out of the system forcing the system renew the boundary layer, while blowing add new fluid flow to the system that renew the boundary layer. An active flow control testing on a Ahmed body showed an improvement in the form of drag reduction. Results from previous study conducted by Haffner et al. [6] pointed out that a drag reduction of 12% was achieved when using a pulsed blowing with coanda deflection surface at four edges of the base. The reduction ratio of the aerodynamic drag by using an air blowing configuration on the head and tail cars of high-speed trains is 9.18%, 12.77%, 10.90%, and 10.78% for the head, middle, tail car, and total train, respectively [7]. A steady on blowing jet test was performed revealed reduction of drag can reach to 29% on a 25° angle Ahmed body. The conditions for the result were an actuator deployed along the upper edge of the rear window which in turn delay the flow separation on the upper edge to downstream of the actuator [8].

An active drag control utilized steady slot jets along the four edges of the base and obtained a maximum drag reduction of 6 %. Further deployed steady blowing with different gas media (helium, air and CO2) near the bottom edge of the base, producing a maximum drag reduction of 11 % when helium was used [9]. A total drag reduction of 6% was achieved using a base blowing through a small, centrally located square aperture at the base of a flat-backed

Ahmed body by research [10]. Tebbiche and Boutoudj achieved drag reduction of 3.6% to 19% with the use of a steady blowing through a micro-hole series at the rear window of Ahmed body [11]. Meanwhile, another research done on the Ahmed body with 25° angle using an unsteady jet. The used of semi-sinusoid jet can make use of suction and blowing depending on the set- up show improvement depending on the set up. The best result it obtains was 12.7% drag reduction by a suction jet with low frequency actuated on the top edge of the angled surface [12]. A total drag reduction up to 3% was achieved experimentally using a series of steady blowing configurations on the global drag past a square back Ahmed bluff body [13].

Table 1 - Summary of active flow control literature review

Research	Active flow control	Location of control	Body	Percentage of drag reduction
Cui W. et al (2015)	Synthetic jet	Upper rear window	Ahmed body	9%
Zhang et al.(2018)	Steady blowing	Upper rear window	Ahmed body	29%
Wang et al (2019)	unsteady jet	The separation part of rear face	Ahmed body	13.6 %
Wang et al.(2019)	Synthetic jet	Upper edge slanted face	Ahmed body	13.6%
Thanh et al (2022)	steady blowing jet	Around the edge rear window	Ahmed body	26.51%
Khan et al (2022)	steady blowing	Center of base	Ahmed body	6%

3. Design

The vehicle is modeled using the idealize automotive body, which is Ahmed body[1], as shown in **Error! Reference source not found.** 2.The Ahmed body axis of the coordinate system are, y axis is parallel to the sides of the body moving from front to the back, x axis is acting from the right side of the body to the left side of the body and Z axis acting from bottom moving upwards direction. **Error! Reference source not found.** 3 shows the geometrical representation of the proposed active control system known as co-flow jet, CFJ. The CFJ blowing and suction slots were located at the slanted surface of the Ahmed body, primarily with the intention of reducing drag. The Ahmed body has dimensions of height, H = 288 mm, length, L = 1044 mm, and width, W = 389 mm. In the present study, the Ahmed body is modelled as a 2-dimensional body, hence it is hanging from the base at d = 50 mm without the supports that represent simplified tires. The suction and blowing jet slots are set up at the locations A and B, respectively.

The height, h, and size, b, of suction and blowing slots is 5 mm and 2 mm, respectively. The momentum coefficient is varied to see its effect on the entrainment of jet fluid into the wake region in the experiment. The momentum coefficient is stated as:

$$C_\mu \frac{lb \ \sin(\Phi + 25)}{BH}\left(\frac{V_j}{U_\infty}\right)^2 = 7.91 \times 10^{-3}$$

(1)

Where, H and B are length and width of the body, l and b are length and width of the slot, Φ is the angle of slot towards rear slant, V_j is the injection jet velocity, U_∞ is the freestream velocity. The blowing/suction velocity is set relative to the freestream velocity, i.e., $V_j = nU_\infty$, where $0 < n < 1$.
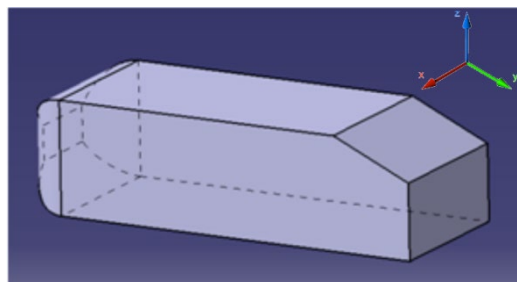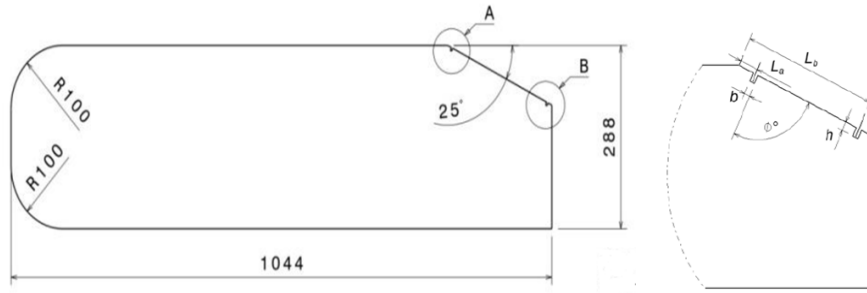

Fig. 2 - Ahmed body

Fig. 3 - Design of CFJ on Ahmed Body. Dimension in mm

4. Variable

There few variables used in the project to be calculated numerically. There are La and Lb, length upper and lower slots from the top of Ahmed body measured parallel to the slanted end, Φ, angle of CFJ slots to the slanted end and then, and injection jet velocity, Vj. The constants variables of the jet slots are b thickness of CFJ slot and h, depth of slot into the body.

Table 2 - CFJ proposed values

Variable (unit)	Proposed Values
L_a (mm)	10, 50, 90
L_b (mm)	150, 210, 270
Φ	90, 122.5, 155
V_j	$0.25U_\infty$, $0.625\,U_\infty$, U_∞
b (mm)	2
h (mm)	5

5. Boundary Condition

From the inlet boundary, a uniform velocity flow, U = 40m/s, while zero reference pressure is imposed at the outlet boundary. The Reynolds number of this analysis, based on model length, is Re = 4.29 × 106. The condition of the bottom walls and Ahmed body is a no- slip condition, while slip condition is imposed on the top wall of the domain. For the 2- dimension computation, an "empty" boundary condition is imposed on the domain lateral walls, whose normal is aligned to geometric directions that do not constitute solution directions. A Neumann boundary condition with zero normal derivatives is imposed on all other boundaries for pressure. Wall functions are imposed on the bottom wall and Ahmed body for turbulence constraints. The numerical domain is shown in Figure 4.
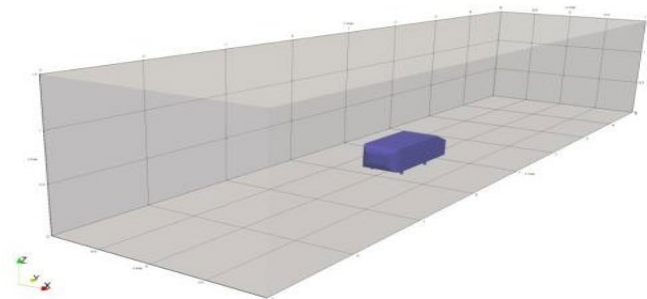

Fig. 4 - Numerical domain

6. Numerical Solver

The governing equations were solved using OpenFOAM software package which will solve the equation by applying Pressure Implicit with Splitting of Operator (PISO) and Semi- Implicit Method for Pressure-linked Equation (SIMPLE) algorithm. The equation for velocity term is calculated by a smooth solver with Gauss-Seidel smoother, while the pressure term is calculated with a generalized geometric-algebraic multi-grid (GAMG) linear solver. Having the three solvers, the Navier-Strokes equations that have incompressible, turbulent flow can be solved correctly than generate a quick solution on a mesh with a small number of cells. As validation cases for the solver used in the present investigation for baseline case, drag coefficients of an Ahmed body at Reynolds number Re = 4.29 × 10^6 were simulated and compared with the data from previous experimental and numerical works.

$$CD = \frac{D}{\frac{1}{2}\rho A V^2} \tag{2}$$

$$CD = \frac{C_D^*}{A V2} \tag{3}$$

Where, D is drag force (N), ρ is density of fluid (1.2 kg/m^3 for air at NTP), A is surface area of the body as viewed from the top (m^2), V is flow velocity (m/s). The values of the drag coefficients CD are shown in Figure 5 as a function of the Reynolds number. A comparison of drag coefficients plotted against Reynolds number, data were obtained from experiments on Ahmed Body from original experiment of Ahmed and al [1] and Meille and al [14] (white triangle and white circle, respectively) and from the present study for the baseline case (blue Square) where CD=0.318 at Re=4.29×10^6. It was observed that the error in drag coefficient decreases with lower Reynolds number. The differences between experimental data and current simulation are likely due to the difference in turbulence intensity and wall functions applied in the simulation.
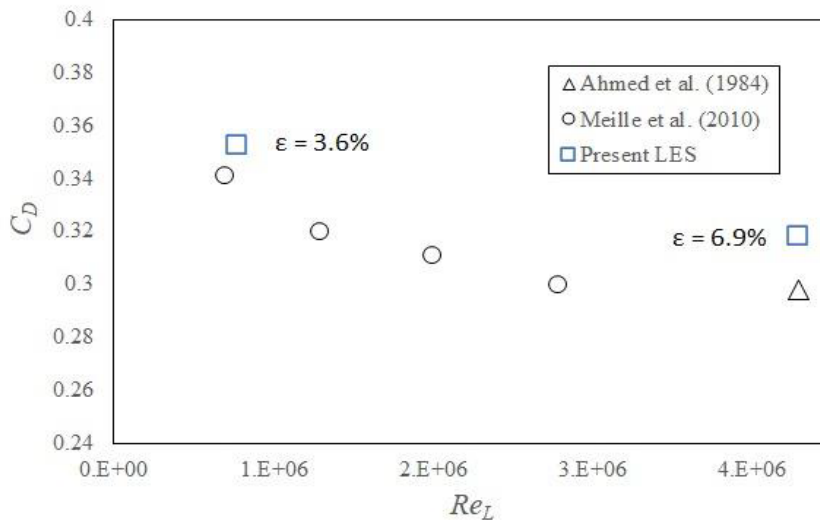

Fig. 5 - Time-averaged drag coefficient plotted against Reynolds number

7. Optimization Study

The application of the response surface methodology (RSM) and central composite design (CCD) was used in the process of optimization and finding the optimum co-flow jet parameters. The parametric study shown that the co-flow jet (CFJ) parameters such as blowing and suction slots locations, velocity jet and slots angle must be optimized to obtain the maximum aerodynamic performance. In our study there are 4 variables (k=4), which are Suction slot location (La), blowing slot location (Lb) , slot angle (Φ) and Coflow jet velocity (Vj). As for surface methodology, this project will use the design of face-centered central composite design combined with RSM. There is also other method of optimization calculation other than CCD in RSM, for example Taguchi method like in the study done to reduce drag on buff body in the year 2013 [15]. However, The Taguchi method can help get close to the bridge but RSM helps to climb the bridge. In another meaning Taguchi's method don't involve all variable combination among input factors. Therefore, RSM is preferred. For 4 or more factors CCD in RSM offers some advantage in requiring a fewer number of runs. CCD is one of the most commonly used structured-design of experiments methods since it is designed to capture corner points of design space which has been used to minimizing both aerodynamic drag and lift of Ahmed body in the year 2017 [16]. Central composite design, CCD can be separated into 3 sub-categories, circumscribed, inscribed and face centered. With careful decision planning, face centered (CCF) was chosen. For face-centered central composite design, $\alpha = \pm 1$, the points are located on the faces of the experimental domain represented by star symbol shown in Figure 6. This variety requires 3 levels of each factor. Face-centered is not a rotatable design.

Table 3 - Design variables

Co-flow jet configuration	La	Lb	Φ	Vj
CFJ1	10	120	90	10
CFJ3	10	200	90	10
CFJ3	10	200	90	40
CFJ5	50	160	90	25
CFJ7	90	120	90	10
CFJ7	90	120	90	40
CFJ9	90	200	90	10
CFJ9	90	200	90	40
CFJ11	10	160	122.5	25
CFJ13	50	120	122.5	25
CFJ14	50	160	122.5	10
CFJ14	50	160	122.5	25
CFJ14	50	160	122.5	40
CFJ15	50	200	122.5	25
CFJ17	90	160	122.5	25
CFJ19	10	120	155	10
CFJ19	10	120	155	40
CFJ21	10	200	155	10
CFJ21	10	200	155	40
CFJ23	50	160	155	25
CFJ25	90	120	155	10
CFJ27	90	200	155	10

To obtain the optimal response of the surface of Ahmed body, mathematical calculation with the application of face-centered central composite design (CCF). The face-centred Central Composite Design is used to determine the number of experiments to be evaluated for the optimization of the variables and responses. The optimum variables will be calculated by Design Expert Software to minimize time-averaged drag coefficient in order to find the desirable points among the results produces. The same software was also used to select the appropriate model to be used. The Fit Summary button displays the sequential F-tests, lack-of-fit tests and other adequacy measures that could be used to assist in selecting the appropriate model. Design Expert Software performs the analysis of variance (ANOVA), post-ANOVA analysis of individual model coefficients and case statistics for analysis of residuals and outlier detection. The analysis and inspection performed in the tests and ANOVA will show whether the model is good or otherwise. Very briefly, a good model must be significant and the lack-of-fit must be insignificant [17]. CCD faced centred design consist of following runs: $2^k + 2k + n_0 = FactorialPoints + Axialpoints + Centerpoints$. In our experiment $k = 4$. The number of factorial runs is $2^4 = 16$, the number of axial points is $2k = 2 \times 4 = 8$ and the number of center points is $n_0 = 3$. Hence, the total runs is $16 + 8 + 3 = 27$.
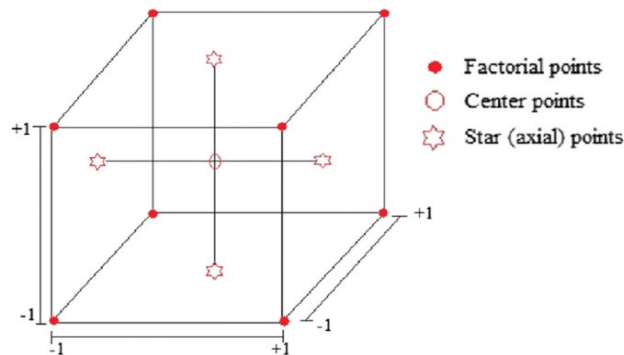

Fig 6 - Face-centered central composite design geometry

8. Results and Discussion

Flows around 2-dimensional Ahmed body with and without Co-flow jet (CJF) have been simulated to investigate the CFJ parameters on the drag experienced by the body. The experiment provide varies results depending on the variables input, whether it is the jet velocity, Vj, location of suction slot, La and blowing slot, Lb, and angle of the slots, Φ. The influence of four studied variables of Coflow jet on Ahmed body can be explained from the 3D response surface plot (Figure 7) and the Design Expert Software results in Table 4. When optimizing the following pair of

parameters, while the other parameter was kept constant at a central point (zero level): (a) Interaction between location of suction slot and location of blowing slot, (b) Interaction between location of suction slot and angle slot, and (c) Interaction between location of blowing slot and jet velocity. Figure 7(a) and Table 4 shows that the optimum suction slot location is observed to be moving through the upper surface of the slant edge and the blowing slot is observed to be moving through the end of the slant edge. Moreover, Figure 7 (a) and (b) demonstrates that the location of suction slot has more impact on the flow than the location of blowing slot and the angle slot. Figure 7(c) show increasing the jet velocity reduces the time-averaged Cd.

Table 4 - Optimization (minimizing time-average Cd) by design expert software

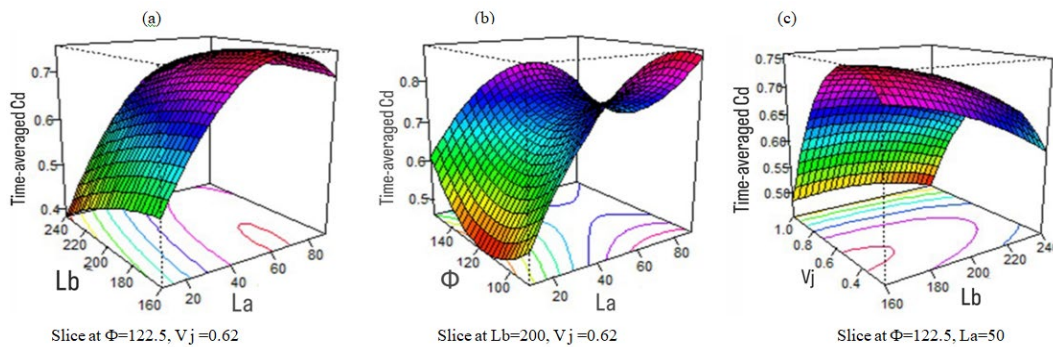| Number	La (mm)	Lb (mm)	Φ (degree)	Vj	Time-Average Cd
1	10	197,25	122,14	0,98	0,262
2	10	169,01	114,68	1	0,291
3	10	187,39	127,32	0,99	0,277
4	10	199,85	122,47	0,93	0,287
5	10	182,38	133,87	1	0,290

Fig 7 - Three-dimensional surface plots

Figure 8 shows plots of time-averaged velocity magnitude for Φ =90° and various La, Lb and Vj; (a) CFJ1V10, (b) CFJ3V10, (c) CFJ3V40, (d) CFJ5V25, (e) CFJ7V10, (f) CFJ7V40. It can be seen in Figure 8 (d-f) that the flow has separated from the Ahmed Body near the upper edge of the slant face. The separation and re-attachment in the upper part of the slant is visible. Next to rear slant there is a pair of counter-rotating vortices, the upper one being significantly larger than the lower one. In cases (a-c) when the distances between the two slots is large and the location of the suction slot is at the upper rear edge the control the flow is virtually completely attached on the slant. The extension of the counter-rotating vortices is increased in downstream direction. This effect due to blows or sucks the boundary layer through slots intensifies the flow in the boundary layer and makes it possible to maintain laminar flow over a large portion of the rear end surface which can significantly reduce frictional resistance and improve the aerodynamic quality of the flow at rear end of the body. For the cases of CFJ 14, with La = 50mm, Lb = 160mm and Φ=122.5°, analyzing the results based on different jet velocity the momentum blowing or suction leads to a delay in the boundary-layer separation, hence a reduction in the pressure drag. Interestingly, increasing Vj from 10m/s to 25m/s and finally 40m/s reduced the $\bar{C}d$ from 0.8267 to 0.7538 then with significant change to 0.2971. By looking into the velocity contour, Fig 9, there are some changes that occur which probably cause by the change in jet velocity. In Fig 9(a), a large dark blue area is clearly visible existing behind the Ahmed body, indicating a significant area of reversed flow region. As the jet velocity increase to 40 m/s (as in Figure 9 (c)), the area of reversed flow decreases significantly on the rear slant and only occur at the vertical rear of the body. It is known that flow separation increases drag on a body due to the low pressure in the reversed flow region.
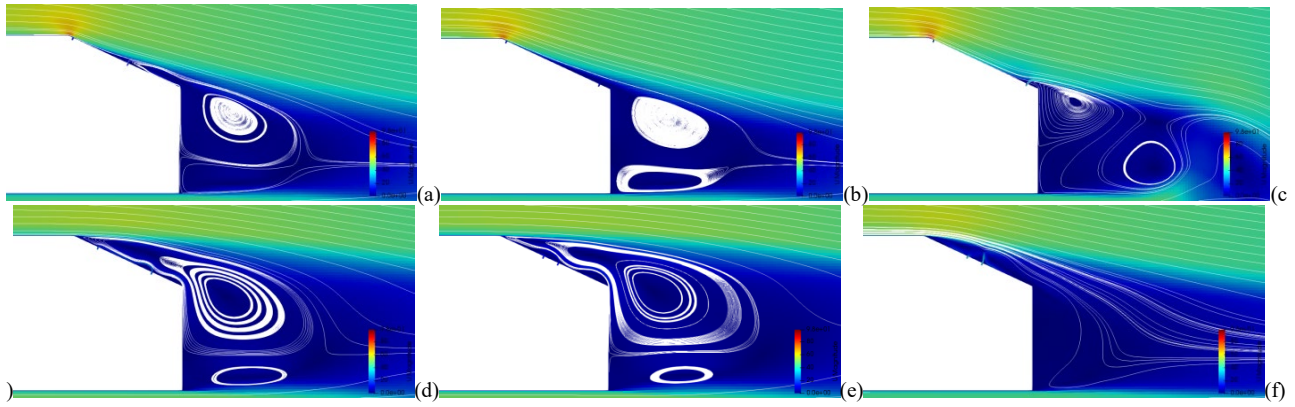
239

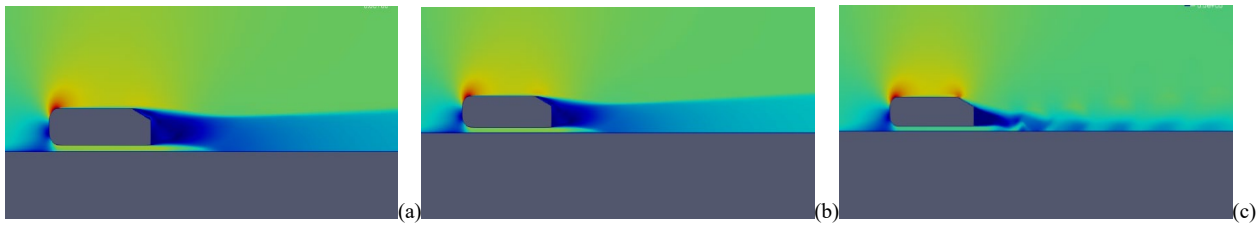**Fig 8 - Time-average velocity magnitude at different location of blowing and suction slots**

Fig 9 - Instantaneous velocity contour of CFJ14 cases (a) 10m/s; (b) 25 m/s; (c) 40m/s

By sorting out the variable results by location of suction slot, La, case of CFJ 11, CFJ14 and CFJ17share jet velocity, Vj = 25m/s, location of blowing slot, Lb = 160mm and angle of slots, φ = 122.5˚, the closer the suction slot to the upper surface, the lower the drag force acting on the body. Where for CFJ17, La is 90mm, giving $\overline{C}d$=0.7980 and for CFJ14, La is 50mm, resulting in $\overline{C}d$=0.7538. It is interesting to note that the $\overline{C}d$ has significantly decreased to 0.3362 for CFJ11 where La is 10mm. For the three cases above, the suction slot location affected the results and decreases the time-average drag coefficient as the suction location is higher on the slant rear of Ahmed body comparing the time-average velocity contour in Figure 10. For CFJ11, the flow is still attached at the rear slant of Ahmed body while the other two cases show flow separation occurs. Suction slot location La proves to be important since the higher the placement of the jet on the slant rear the drag coefficient decreases. This is similar to the conclusion came out for paper by M.Jahanmiri[18].

For CFJ19 and CFJ21, which share the same suction slot location, La=10mm and angle of slots, φ=155˚ but different in terms of locations of blowing slot Lb, which are 120mm and 200mm, respectively. From the 2D analysis, it was found that the closer the blowing slot to the end of the rear edge, the lower the time-averaged drag coefficient for both jet velocities of 10m/s and 40m/s. The time-averaged drag coefficients have decreased by approximately 48% and 31% for Vj = 10 m/s and 40 m/s, respectively. It is observed that the impact of blowing slot location is more apparent for lower jet velocity or lower jet momentum coefficient. Upon inspection of Figure 11, it can be clearly seen that the blowing jet in CFJ21 has successfully delayed the separation, while locating the blowing slot closer to the upper edge of the rear slant surface (i.e. CFJ19) resulted in earlier separation. Worth mentioning the surface pressure acting at rear slant and end are higher with CFJ 19 compared to CFJ21 as can be seen in Fig1. This result confirms findings reported by Xavier [19].
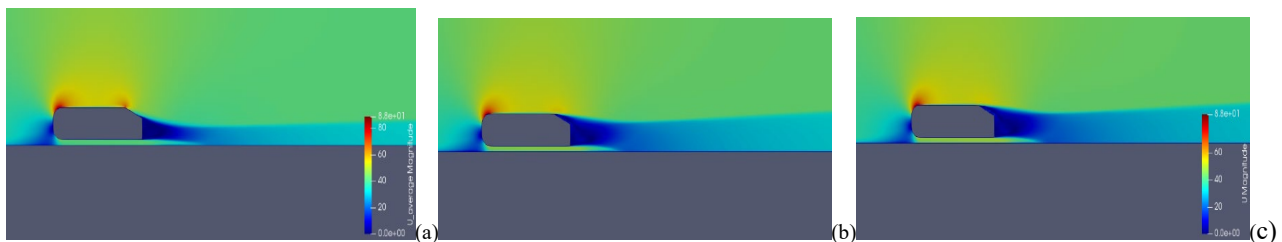

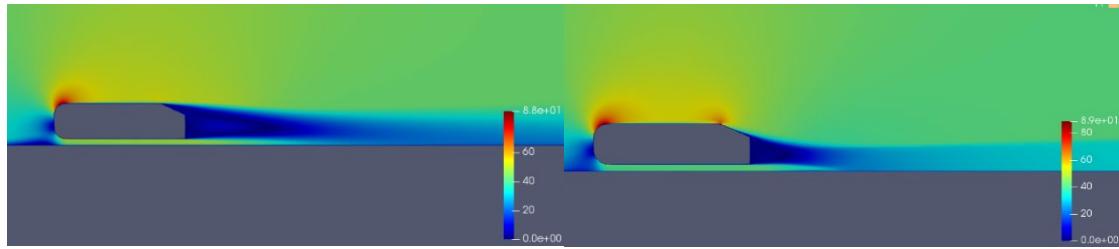**Fig. 10 - Time-average velocity contour with different La (a) 10; (b) 50; (c) 90**

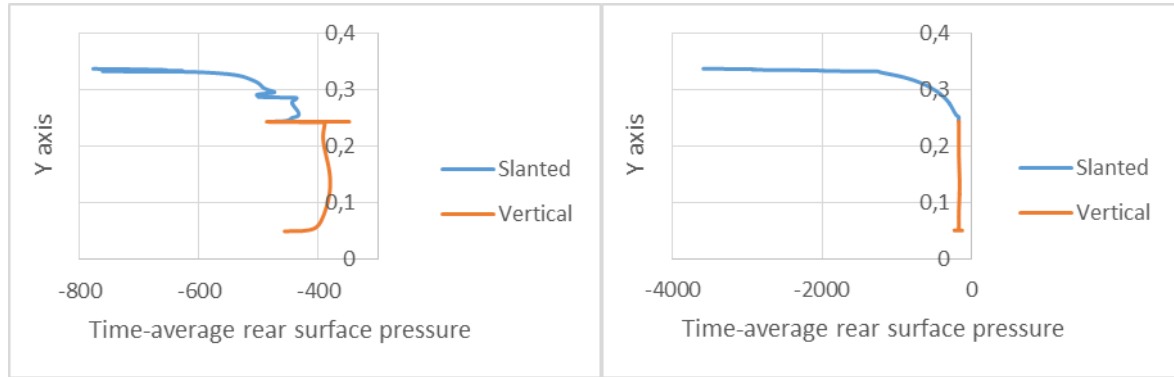**Fig. 11 - Time-average velocity contour with different Lb, (left) 120 (right) 200**
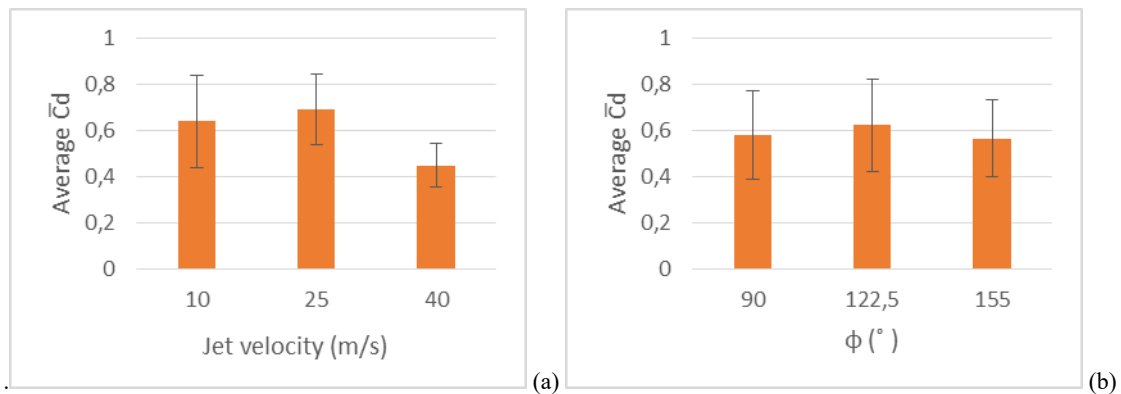

Fig. 12 - Time-average surface pressure of rear end VS Y-axis graph with different Lb, (left) 120 (right) 200

In Fig3 (a), the graphs are adjusted into four variables of jet velocity, angle of slot, location of suction slot and location of blowing slot. By inspecting the jet velocity graph, the average $\bar{C}d$ for jet velocity 40m/s is clearly smaller compared to 10m/s and 25m/s. Even when comparing the standard deviation, when the jet velocity 10m/s cases is higher than for 40m/s cases, which is due to the larger difference between minimum and maximum drag coefficient in its data. This is probably due to the fact that most of the previous cases using jet velocity 40 m/s have a lower time-averaged drag coefficient $\bar{C}d$. A trend was observed for the average by location of suction slot value of $\bar{C}d$, in Fig3 (c). When the suction slot location is at 10mm from the top, the average $\bar{C}d$ is 0.4237, which is significantly lower than when location of suction slot at 50mm or 90mm from the top surface. Similar with the jet velocity cases, the standard deviation for suction slot location 10mm is smaller compared to others. The smaller difference between maximum and minimum time-average drag coefficient, $\bar{C}d$ in suction slot location 10mm are the reason for the smaller standard deviation. For the location of blowing slot, having it be further end of the slanted rear, Lb = 200mm, decrease the average $\bar{C}d$ then having it closer to the top at 120mm and 160mm. Although, the standard deviation for all three dimensions is almost similar, in Fig3(d). The fact is that few more cases that used blowing slot at a lowest location, Lb = 200mm have produced smaller $\bar{C}d$ can be taken into consideration.

However, out of all the variables used in the study, angle of slot shows only minuscule changes towards the time-average drag coefficient, $\bar{C}d$. Having almost similar average $\bar{C}d$ and standard deviation throughout all the different dimensions of data as shown in Fig13(b). As a whole no considerable effect of blowing slot location and slot angle is observed. However, it is clear that the suction slot location at the upper edge and jet velocity 40m/s decreases the drag coefficient. As the suction slot location becomes closer to the upper edge and the jet velocity increase to 40m/s, the average $\bar{C}d$ decrease. Increasing jet intensity reduces the drag coefficient.
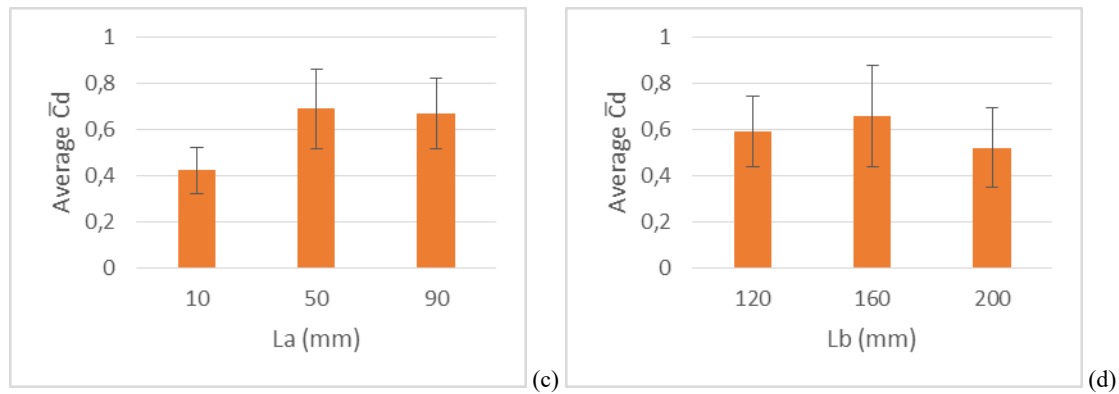

(a)   (b)

(c)   (d)

Fig. 13 - Average time-averaged drag coefficient and standard deviation (a) by jet velocity, Vj; (b) by angle of slot, Φ; (c) by position of slot A, La; (d) by position of slot B, Lb

9. Conclusion

The effects of suction and blowing jet at the slanted rear of an Ahmed body on the drag reduction has been investigated. Independent variables include co-flow jet velocity, position of co-flow jet and angle of co-flow jet. It was found that under certain configurations, the co-flow jet can unsteadiness in the wake flow. Furthermore, the velocity of the jet played a pivotal point on the condition of the flow. Worth mentioning is that out of all the variables, increasing the jet velocity are the most effective method of reducing drag. This is due to the fact that an increase in jet velocity (particularly suction) removes the boundary layer more effectively, thus delaying the onset of flow separation and ultimately reducing the drag. While position of both suction and blowing jet also provide better understanding that the higher the suction jet and the lower the blowing jet, the better the drag reduction is. However, out of all the variables, the angle of the slot, does not show any importance in reducing drag compared with other variables. Therefore, the application of suction and blowing jet as an active flow control is applicable when the jet velocity and location of jet are adjusted appropriately.

Acknowledgement

References

[1] S. R. Ahmed, G. Ramm, and G. Faltin, *Some salient features of the time - averaged ground vehicle wake*, vol. 840300. 1984.

[2] S. Shadmani, S. M. Mousavi Nainiyan, R. Ghasemiasl, M. Mirzaei, and S. G. Pouryoussefi, "Experimental study of flow control over an ahmed body using plasma actuator," *Mech. Mech. Eng.*, vol. 22, no. 1, pp. 239-251, 2018.

[3] M. Gad-el-Hak, "Flow control: The future," *J. Aircr.*, vol. 38, no. 3, pp. 402-418, 2001.

[4] K. Yousefi and R. Saleh, "Three-dimensional suction flow control and suction jet length optimization of NACA 0012 wing," *Meccanica*, vol. 50, no. 6, pp. 1481-1494, 2015.

[5] A. Altaf, A. A. Omar, and W. Asrar, "Review of Passive Drag Reduction Techniques for Bluff Road Vehicles," *IIUM Eng. J.*, vol. 15, no. 1, pp. 61-69, 2014.

[6] Haffner, Y., Borée, J., Spohn, A. & Castelain, T. "Unsteady Coanda effect and drag reduction for a turbulent wake". J. Fluid Mech. 899, A36, 2020.

[7] Z. Wei Chen, G. Zhi Zeng, Y. Qing Ni, T. Hong Liu, J. Qiang Niu, H. Dong Yao, Reducing the aerodynamic drag of high-speed trains by air blowing from the nose part: Effect of blowing speed, vol. 238. Elsevier B.V., 2023.

[8] B. F. Zhang, K. Liu, Y. Zhou, S. To, and J. Y. Tu, "Active drag reduction of a high-drag Ahmed body based on steady blowing," pp. 351-396, 2018.

[9] Lorite-Díez, M., Jiménez-González, J.I., Pastur, L., Martínez-Bazán, C. & Cadot, O. "Experimental analysis of the effect of local base blowing on three-dimensional wake modes". J. Fluid Mech. 883, A53,2020.

[10] Khan, T.I., Parezanović, V., Pastur, L. & Cadot, "Suppression of the wake steady asymmetry of an Ahmed body by central base bleed". Phys. Rev. Fluids 7 (8), 083902, 2022.

[11] *H. Tebbiche, M.S. Boutoudj,"Active flow control by micro-blowing and effects on aerodynamic performances. Ahmed body and NACA 0015 airfoil",Int. J. Fluid Mech. Res., pp. 29-46,2021.*

[12] B. xin Wang, Z. gang Yang, and H. Zhu, "Active flow control on the 25°Ahmed body using a new unsteady jet," *Int. J. Heat Fluid Flow*, vol. 79, no. November 2018, 2019.

[13] Plumejeau, L. Keirsbulck, J. Basley, M. Lippert, S. Delprat, W. Abassi, Drag mitigation by steady blowing and Coanda effect on a square back Ahmed body, vol. 98. Elsevier B.V., 2023..

[14] *W. Meile, G. Brenn, A. Reppenhagen, B. Lechner, and A. Fuchs, "Experiments and numerical simulations on the aerodynamics of the ahmed body," CFD Lett., 2011.*

[15] S. H. Seo, C. Do Nam, J. Y. Han, and C. H. Hong, "Drag reduction of a bluff body by grooves laid out by design of experiment," *J. Fluids Eng. Trans. ASME*, vol. 135, no. 11, 2013.

[16] K. Song, K. H. Choo, J.-H. Kim, and D. N. Mavris, "MULTI-OBJECTIVE DECISION MAKING OF A SIMPLIFIED CAR BODY SHAPE TOWARDS OPTIMUM AERODYNAMIC PERFORMANCE," in *Proceedings of the ASME 2017 International Design Engineering Technical Conferences and Computers and Information in Engineering Conference*, 2017, pp. 1-9.

[17] M. S. Said *et al.*, "Comparison between Taguchi Method and Response Surface Methodology (RSM) In Optimizing Machining Condition Department of Mechanical & Materials Engineering , Faculty of Engineering and Built Environment ," *Int. Conf. Robust Qual. Eng.*, pp. 60-64, 2013.

[18] M. Jahanmiri and M. Abbaspour, "Experimental investigation of drag reduction on Ahmed car model using a combination of active flow control methods," *Int. J. Eng. Trans. A Basics*, 2011.

[19] P. Joseph, X. Amandolèse, and J. L. Aider, "Drag reduction on the 25° slant angle Ahmed reference body using pulsed jets," *Exp. Fluids*, vol. 52, no. 5, pp. 1169-1185, 2012.